Comparison of the biomechanical tensile and compressive properties of decellularised and natural porcine meniscus

A. Abdelgaied [a,*], M. Stanley [a], M. Galfe [b], H. Berry [b], E. Ingham [c], J. Fisher [a]

[a] Institute of Medical and Biological Engineering, School of Mechanical Engineering, Leeds LS2 9JT, UK
[b] Tissue Regenix, York, UK
[c] School of Biomedical Sciences, University of Leeds, Leeds, UK

ABSTRACT

Meniscal repair is widely used as a treatment for meniscus injury. However, where meniscal damage has progressed such that repair is not possible, approaches for partial meniscus replacement are now being developed which have the potential to restore the functional role of the meniscus, in stabilising the knee joint, absorbing and distributing stress during loading, and prevent early degenerative joint disease. One attractive potential solution to the current lack of meniscal replacements is the use of decellularised natural biological scaffolds, derived from xenogeneic tissues, which are produced by treating the native tissue to remove the immunogenic cells. The current study investigated the effect of decellularisation on the biomechanical tensile and compressive (indentation and unconfined) properties of the porcine medial meniscus through an experimental–computational approach. The results showed that decellularised medial porcine meniscus maintained the tensile biomechanical properties of the native meniscus, but had lower tensile initial elastic modulus. In compression, decellularised medial porcine meniscus generally showed lower elastic modulus and higher permeability compared to that of the native meniscus. These changes in the biomechanical properties, which ranged from less than 1% to 40%, may be due to the reduction of glycosaminoglycans (GAG) content during the decellularisation process. The predicted biomechanical properties for the decellularised medial porcine meniscus were within the reported range for the human meniscus, making it an appropriate biological scaffold for consideration as a partial meniscus replacement.

1. Introduction

The meniscus is recognised as having an important role in stabilising the knee joint (Allen et al., 2000), as well as redistributing (Kurosawa et al., 1980; Voloshin and Wosk, 1983) and reducing stress during loading (Fukubayashi and Kurosawa, 1980; Ahmed and Burke, 1983; Ahmed et al., 1983). The shock absorption effect of meniscus has recently been discussed (Andrews et al., 2011). The meniscus also plays an important role in joint lubrication and nutrient distribution (Allen et al., 1995). Excessive harmful deformation is controlled by the "stress stiffening" feature of the collagen-fibre structure of the menisci (Rongen et al., 2014).

Tearing of the meniscus is one of the most common injuries of the knee (Baratz et al., 1986; Muscolo et al., 2006), with a high risk of subsequent degenerative changes within the joint if the meniscus is removed (Aagaard and Verdonk, 1999; Englund et al., 2003; Mcdermott and Amis (2006); Stensrud et al., 2014). Meniscal repair is now widely adopted as a treatment for meniscus injury (Laible et al., 2013; Moriguchi et al., 2013; James et al., 2014). If meniscal repair is, however, not possible, partial meniscus replacement can be performed in order to maintain the functional role of the meniscus with the aim to prevent early degenerative joint disease (Papalia et al., 2013).

Meniscal allografts have been used to replace the meniscus since the 1980s (Milachowski et al., 1989; Stollsteimer et al., 2000; Wirth et al., 2002; Faivre et al., 2014; Vundelinckx et al., 2014; Yoon et al., 2014). Although allograft tissues are sterilised using different sterilisation methods to prevent potential problems of disease associated with allograft transplantation (Kainer et al., 2004; Tugwell et al., 2005), allograft transplantation is still constrained by the limited availability of donor tissue of suitable quality. Biomaterials, both natural and synthetic are being researched and developed with a view to constructing a meniscal implant or a cell-seeded scaffold capable of restoring the major functions of the meniscus. Ideally these devices or engineered tissues should have a structure similar to the fibro-cartilaginous structure to the native meniscus in order to restore load-transfer function (Marsano et al., 2006; Kon et al., 2008,

* Correspondence to: Institute of Medical and Biological Engineering, School of Mechanical Engineering, University of Leeds, Room X301, Leeds LS2 9JT, UK. Tel.: +44 113 343 9089; fax: +44 113 242 4611.
E-mail address: A.Abdelgaied@leeds.ac.uk (A. Abdelgaied).

2012). To date, however, this has not been achieved using synthetic or natural biomaterials.

One potential solution to the current lack of suitable meniscal replacement/repair devices is the use of decellularised natural xenogeneic tissue which is produced by treating the native tissue to remove the immunogenic cells (Stapleton et al., 2008). Decellularised natural xenogeneic tissues can provide an "off the shelf" solution, are not constrained by donor tissue supply and can be translated to the clinic as class 3 medical devices. Preservation of the native tissue structure and biomechanical properties during the process of decellularisation of the tissue is highly desirable, to enhance meniscus repair function. The use of an off the shelf decellularised scaffold derived from porcine tissue offers the potential for supplying a product range of different sizes, as well as allowing the surgeon to prepare the size and geometry (shape) intra-operatively. This provides potential for greater flexibility in both supply, sizing and matching of geometry compared to the limited supply of donor allograft tissues currently used.

The aim of the current study was to investigate the effect of decellularisation on the tensile and compressive biomechanical properties of the porcine medial meniscus through an experimental–computational study.

2. Materials and methods

Native and decellularised porcine medial menisci were supplied by Tissue Regenix Group Plc, York, UK. The animals used in the current study were typically six months old and weighed between 90 and 105 kg. Native porcine meniscus was decellularised by exposing the tissue to freeze-thaw cycles, incubation in hypotonic tris buffer, 0.1% (w/v) sodium dodecyl sulfate in hypotonic buffer plus protease inhibitors, nucleases, hypertonic buffer followed by disinfection using 0.1% (v/v) peracetic acid and final washing in phosphate-buffered saline, according to the decellularisation protocol published elsewhere (Stapleton et al., 2008). Decellularised meniscus samples were prototypes, not final product, and they were aseptically processed but not terminally sterilised. Native and decellularised menisci were stored frozen until mechanical testing. Although many studies on native animal and human tissues have reported that low number of freezing—thawing cycles (less than three cycles) did not affect neither macroscopic (Proctor et al., 1989) nor the biomechanical properties (Maroudas et al., 1968; Athanasiou et al., 1991; Yahia and Zukor, 1994; Huang et al., 2011) of the tissue, there are conflicting opinions of the effects of freezing on the biomechanical properties of native tissues (Hori and Mockros, 1976). Freezing may affect the viability of cells in native menisci, however, our data on testing fresh and frozen porcine menisci using the creep indentation tests showed no difference between the frozen meniscus used in the current study and fresh meniscus ($n=9$ specimens). Therefore, in order to maintain a similar pre-test storage condition to the decellularised menisci, the native menisci were stored frozen until mechanical testing. Moreover, the number of freezing—thawing cycles for both native and decellularised menisci was one cycle. All the mechanical tests were performed according to standard operating procedures (SOP) developed specifically for the meniscus.

2.1. Tensile tests

Mechanical uniaxial tensile tests were conducted, using an Instron uniaxial testing instrument, to determine the tensile initial elastic modulus, elastic modulus, transition stress, transition strain and ultimate tensile strength of each specimen. The tests were conducted at approximately 20 °C and 1 mm/min with strain rate of 0.00167 s^{-1}, similar to that was used by Proctor et al. to negate the frictional drag effects caused by interstitial fluid flow (Proctor et al., 1989), and similar to what was reported for tensile tests of meniscus (Fithian et al., 1990; Goertzen et al., 1997; Lechner et al., 2000). The low strain rate used in the current study is not physiologically representative (Chia and Hull, 2008) but was selected in order to obtain more consistent determination of failure properties in tension. A higher strain rate would produce larger drag forces that would help support the load while at equilibrium stresses are supported solely by the solid matrix (Chia and Hull, 2008). In addition, constant strain-rate ramp tests conducted at extremely slow strain rates could possibly allow viscoelastic dissipation and, hence, yield the elastic material properties of the tissue (Lynch et al., 2003). The test specimens were gripped using custom made adjustable wide titanium grips to allow better stress distribution over a wider gripping area. The bottom part of the grip was used to apply a pre-load of 0.5 N (the weight of lower part of the grip), no further pre-load was applied. The strain was measured from grip to grip and marker points were added at the tissue—grips edges to monitor the tissue slippage. The specimens

which slipped during the test were discarded from the analysis. The meniscal specimens were kept hydrated for the duration of the tests using phosphate buffered saline (PBS) spray. On the day of testing, slices were cut frozen from the central portion of the menisci to the pre-specified thickness, using a custom made tissue cutter. The tensile test specimens were then cut from the middle portion to the pre-specified width and were initially rectangle-shaped. However, to reduce the high number of specimen failures that occurred at the grips (more than 50%) in the rectangular specimens, the tensile test specimens were then cut with a dumbbell-shape with a gauge length of 10 mm between the grips (Fig. 1). Five different native meniscal specimens with cross-sectional areas of 1.5×1.5, 1.5×3, 2×3, 3×2 and 3×3 [mm] (thickness × width) were tested to represent different meniscal regions (with different structures) (Fox et al., 2012). However, based on the sensitivity study on native meniscus, decellularised meniscal tensile specimens of 3×3 [mm] cross-sectional area were used. The specimens' dimensions were checked and only specimens with dimensions within $\pm 10\%$ of the pre-specified dimensions were considered. The specimens were kept hydrated during preparation using PBS.

The experimental stress strain data were processed in Matlab (Matlab R2011b). The initial elastic modulus and elastic modulus were defined as the slope of the linear curve fit up to 1% strain and the slope of the linear part of the curve, based on the best R-square value using the linear curve fitting and optimisation functions in Matlab (Matlab R2011b), respectively. The intersection point of the two slopes defined the transition stress and strain. The ultimate tensile strength was defined as the highest point on the stress strain curve, as shown in Fig. 1.

2.2. Indentation creep tests

Mechanical creep indentation tests were conducted using cylindrical specimens (meniscal pins) to determine the indentation elastic modulus, permeability and Poisson's ratio of each specimen (Fig. 2). Each meniscal pin was subjected to creep-deformation at approximately 20 °C using a 2.5 mm rigid flat indenter under 0.05 MPa stress. The instantaneous (within 40 ms) load was maintained until the creep deformation reached equilibrium. The test times were 3600 and 4800 [s] for native and decellularised meniscus respectively, during which creep deformations were recorded. The instance at which the full load was recorded was assumed to be the start time ($t=0$). The meniscal pins were kept submerged in PBS for the duration of the test.

On the day of testing, 8 mm diameter cylindrical specimens were cut from the central portion of the anterior, middle and posterior sections of the menisci and were then cut to the specified thickness (Fig. 2). Five different native meniscal specimens of 0.5, 1, 1.5, 2 and 3 [mm] thicknesses were tested. However, based on the sensitivity study on native meniscus and to represent different meniscal regions, two different decellularised meniscal pin thicknesses of 1.5 and 3 [mm] were tested. The specimens were kept hydrated during preparation using PBS. The specimens' dimensions were checked prior to testing, after at least 30 min in PBS, based on the sensitivity study on the effect of PBS absorption on the specimen dimensions, and only specimens with dimensions within $\pm 10\%$ of the pre-specified dimensions were considered.

The linear-biphasic indentation creep problem was solved using a combined analytical and computational approach. This solution scheme allowed simultaneous computation of the three independent intrinsic biphasic properties of the menisci. The shear modulus was first calculated using the equation derived from the solution by Hayes et al. (1972) and an initially assumed Poisson's ratio (Poisson's ratio of zero was initially assumed, to allow for maximum biphasic effect (Jin et al., 2000); however, this value is updated through the iteration process). The elastic modulus of the solid matrix was then calculated. A finite
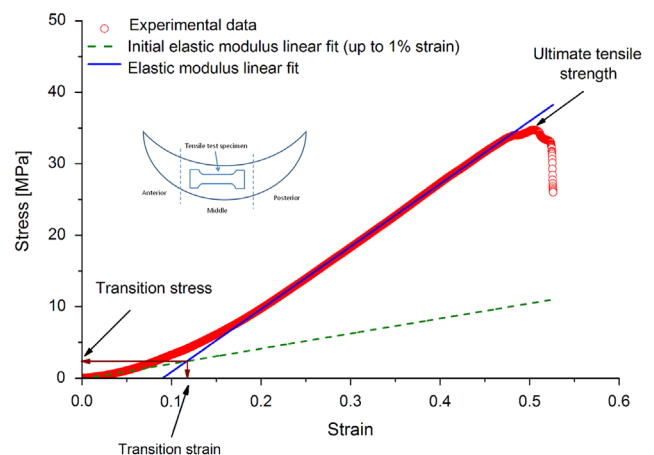

Fig. 1. Representative curve for the tensile test, test specimen, and different tensile biomechanical properties.
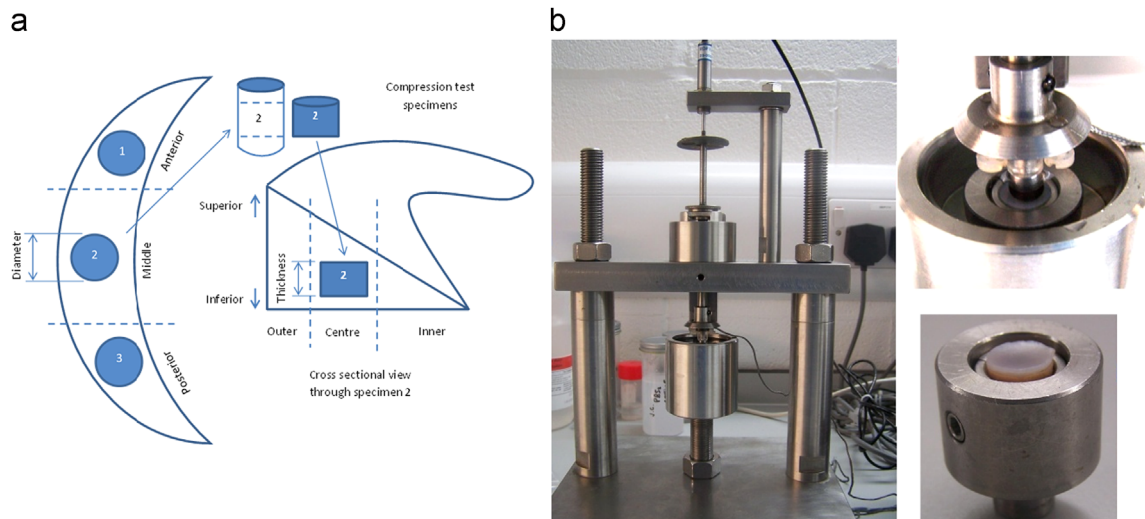
Fig. 2. Right medial meniscus showing the specimen locations (a) and the indentation and unconfined test rig (b).

element (FE) model of the indentation problem was created in ABAQUS (SIMULIA, ver. 6.12-2). The solution algorithm described by Pawaskar et al. (2010) was used to solve, for the meniscal pin, permeability and Poisson's ratio, assuming 74% water content (Fithian et al., 1990; Joshi et al., 1995; Sweigart et al., 2004). However, the effect of water content on the predicted biomechanical properties was investigated. The predicted new value for the Poisson's ratio from the FE model was then used to calculate the new elastic modulus of the solid matrix. This iteration process continued until the best R squared value between the experimental and the computational deformations was obtained. The described solution scheme allowed simultaneous computation of the three independent intrinsic biphasic properties of soft tissue. Indentation compression creep tests were conducted to determine the equivalent (full creep curve was considered) and equilibrium (only the final 30% creep deformation was considered) compressive biomechanical properties of each specimen.

2.3. Unconfined compression test

On the day of testing, 8 mm diameter cylindrical specimens were cut frozen from the central portion of the anterior, middle and posterior sections of the menisci, and were then cut to the specified thickness (Fig. 2). The unconfined compression creep study was run using 3 mm thickness meniscal pins, to describe the overall structure of the tissue. The specimens were kept hydrated during preparation using PBS. The specimens' dimensions were checked prior to testing, after at least 30 min in PBS, based on the sensitivity study on the effect of PBS absorption on the specimens' dimensions, and only specimens with dimensions within ± 10% of the pre-specified dimensions were considered (maximum of 3 meniscal pins out of 18 were not within the ± 10%, for 3 mm thickness decellularised meniscus, and were therefore discarded).

Mechanical unconfined compression creep tests were conducted to determine the unconfined elastic modulus and permeability of each specimen. Each meniscal pin was subjected to unconfined creep-deformation at approximately 20 °C using two rigid smooth flat plates under 0.01 and/or 0.05 [MPa] stresses. The instantaneous (within 40 ms) load was maintained until the creep deformation reached equilibrium. The test time was 3600 s, during which creep deformations were recorded. The instance at which the full load was recorded was assumed to be the start time ($t=0$). The meniscal pins were kept submerged in PBS for the duration of the test.

The biphasic unconfined compression creep problem was solved using the linear biphasic solution formulated by Armstrong et al. (1984). The solution algorithm was developed in Matlab (Matlab R2011b) and was used to solve for the meniscal pin permeability and elastic modulus, assuming 74% water content and Poisson's ratio of zero or 0.1 (Sweigart et al., 2004). The calculated permeability and elastic modulus were iterated to match the calculated creep values to the experimental measurements. This iteration process continued until the best R squared value between the experimental and the computational deformations was obtained. Unconfined compression creep tests were conducted to determine the equivalent (full creep curve) and equilibrium (final 30% creep deformation) compressive biomechanical properties of each specimen.

2.4. Data analysis

All numerical data were analysed using SPSS statistics (IBM SPSS, ver. 22). The means and outliers within each set of data were calculated using the Descriptive Statistics function with 95% confidence interval. Data from fresh and decellularised specimens as well as data from different test configurations were compared using the one-way analysis of variance (ANOVA). When necessary, a Post-hoc test was performed (Fisher's Protected Least Significant Difference (LSD), Tukey and Gabriel tests). A p-value < 0.05 was accepted as significant. In addition, the statistical analysis was cross-checked in Matlab using an in-house developed statistical program (Matlab R2011b).

3. Results

3.1. Tensile tests

Representative curve for the tensile test results is shown in Fig. 1. When the dumbbell-shaped specimens were used, more than 75% failures occurred within the middle of the test specimens. Specimens which failed at the grips were discarded from the analysis and only the results for those which failed at their central regions were considered. The tensile biomechanical properties for native meniscus are shown in Fig. 3. The sensitivity study on the native meniscal cross-sectional area of the tensile test specimens showed a dependence of the tensile biomechanical properties on the cross-sectional area of the tensile specimen. However, this dependence was found not to be statistically significant in the majority of the comparisons of the groups (only the differences in the measured ultimate strength and transition strain between 1.5×1.5 and 3×3 [mm] (thickness × width) specimens and in the measured initial elastic modulus between 1.5×1.5 and 3×2 [mm] (thickness × width) specimens were significantly different (ANOVA, $p < 0.05$)). Therefore recommendation for future testing was to use 3×3 [mm] (thickness × width) specimens, to describe the overall structure of the tissue. The measured initial elastic modulus, elastic modulus, ultimate tensile strength, and transition stress for the native porcine meniscus were in the ranges 14 to 26, 113 to 142, 23 to 33, and 2 to 3.2 [MPa] respectively, depending on the cross-sectional area of the meniscal samples. The corresponding transition strain ranged between 4.6 and 6.4% strain.

The tensile biomechanical properties of decellularised medial porcine meniscus are compared to that of native medial porcine, using meniscal specimens of 3×3 [mm] cross-sectional area, in Fig. 4. The decellularised scaffold showed lower initial elastic modulus (9.41 ± 1.38) (ANOVA, $p < 0.05$), compared to that of native porcine meniscus. The measured elastic modulus (133 ± 11), ultimate strength (35 ± 4.5), transition stress (1.66 ± 0.23), and transition strain (5.32 ± 0.58) for the decellularised porcine meniscus were,
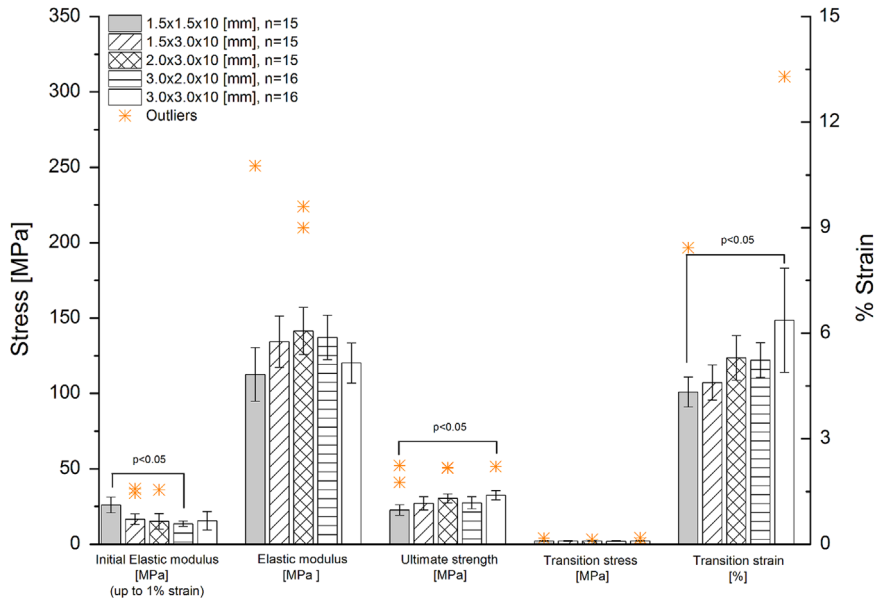
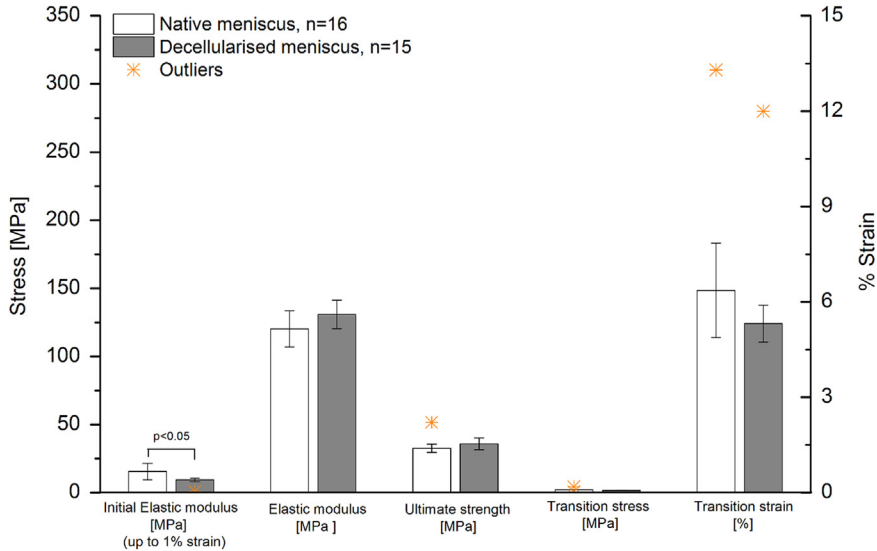**Fig. 3.** Tensile mechanical properties for native menisci (mean $\pm$ 95% CI) at 0.00167 s^{-1} strain rate.

Fig. 4. Tensile mechanical properties for native and decellularised menisci ($3.0 \times 3.0 \times 10$ [mm] samples, mean $\pm$ 95% CI) at a strain rate of 0.00167 s^{-1}.

however, not significantly different (ANOVA, $p > 0.05$, $n \geq 15$) compared to that of native meniscus.

3.2. Indentation creep tests

Representative curve for the compressive creep test results is shown in Fig. 5. The sensitivity study showed no further change in the specimens' dimensions, due to PBS absorption, after 30 min and up to 5 h. The sensitivity analysis on the native meniscal pin thickness of the compressive creep indentation test specimens showed that specimens of 1.5 mm thickness were sufficient to describe the biomechanical properties of the tissue (ANOVA, $p > 0.05$). In addition, the indentation creep results showed no significant differences between the anterior, middle and posterior meniscal regions (ANOVA, $p > 0.05$), as shown in Table 1. Moreover, the effect of meniscus water content (from 60% to 80%) on the predicted properties from the computational simulation model was shown to be insignificant. Similar finding was reported by Abd Latif et al. (2012).
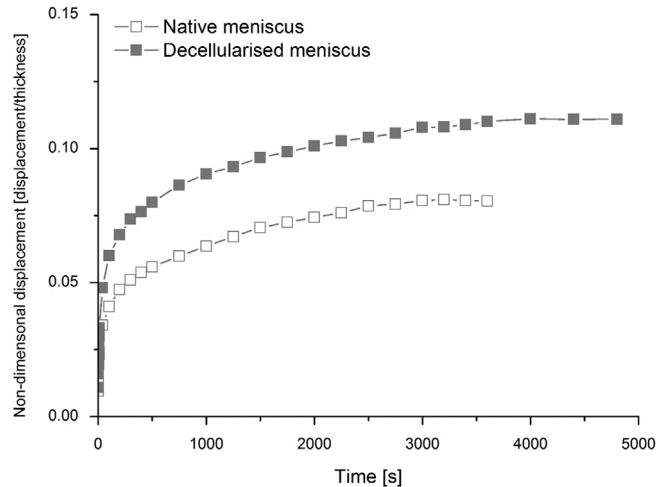

Fig. 5. Representative curve for the compressive creep test results, 3 mm thickness meniscal pins and 0.05 MPa stress indentation test.

The predicted Poisson's ratio for native and decellularised menisci was zero. The predicted equivalent elastic modulus and permeability for the 1.5 and 3 [mm] thickness native meniscus are summarised in Table 2. Only the predicted equivalent elastic moduli for the 1.5 mm specimens of the native and decellularised tissues were significantly different (ANOVA, $p < 0.05$).

3.3. Unconfined compression test

The sensitivity study showed no further change in the specimens' dimensions, due to PBS absorption, after 30 min and up to 5 h. The unconfined compression creep tests were first run under 0.05 MPa stress, similar to the indentation creep study. However, high creep deformations were measured (creep deformation > 25% meniscal pin's thickness), therefore the unconfined compression creep study was run under 0.01 MPa stress to maintain low deformation levels to match the linear biphasic theory and constant permeability assumptions used in the current study (Armstrong et al., 1984). The measured deformation levels under the 0.01 MPa stress, of approximately 8% and 11% of the specimen thickness for native and decellularised menisci respectively, were within the deformation ranges reported with the linear biphasic solution (Proctor et al., 1989; Athanasiou et al., 1991). The predicted equivalent elastic modulus and permeability for zero Poisson's ratio were 0.12 ± 0.03 MPa and $2.07 \times 10^{-15} \pm 0.24 \times 10^{-15}$ m^4/N s, and 0.09 ± 0.02 MPa and $2.47 \times 10^{-15} \pm 0.27 \times 10^{-15}$ m^4/N s (mean $\pm$ 95% CI) for native and decellularised meniscus, respectively. Similar values and trend were predicted for equilibrium and for 0.1 Poisson's ratio as well, as shown in Fig. 6. The predicted elastic moduli for native and decellularised tissues were not significantly different (ANOVA, $p > 0.05$). However, the difference between the predicted equilibrium permeability for native and decellularised menisci with 0.1 Poisson's ratio was significant (ANOVA, $p < 0.05$).

4. Discussion

Partial meniscus replacement devices may be used clinically to prevent secondary osteoarthritis in the knee joint. These devices should ideally have similar intrinsic biomechanical properties to native meniscus, to enable function of the partial meniscus replacement to be delivered, and be capable of fully supporting tissue neogenesis (Rizzi et al., 2012). An decellularised scaffold derived from natural xenogeneic tissue is one potential solution (Stapleton et al., 2008). The effect of the decellularisation process on the biomechanical properties of the meniscus requires in depth investigation. The current study therefore investigated the effect of decellularisation on the tensile and compressive biomechanical properties of the porcine medial meniscus.

Table 1
Equivalent biomechanical properties for different specimens' locations of native porcine menisci (mean $\pm$ 95% CI), for 1.5 mm thickness meniscal pins and 0.05 MPa stress indentation test.

	Anterior ($n=5$)	Centre ($n=6$)	Posterior ($n=5$)
E [MPa]	0.24 ± 0.095	0.23 ± 0.101	0.25 ± 0.089
Permeability [$\times 10^{-15}$ m^4/N s]	4.04 ± 2.33	3.79 ± 2.31	3.46 ± 2.16

Table 2
Indentation biomechanical properties for native and decellularised porcine menisci (mean $\pm$ 95% CI), for 1.5 and 3 [mm] thickness meniscal pins and 0.05 MPa stress.

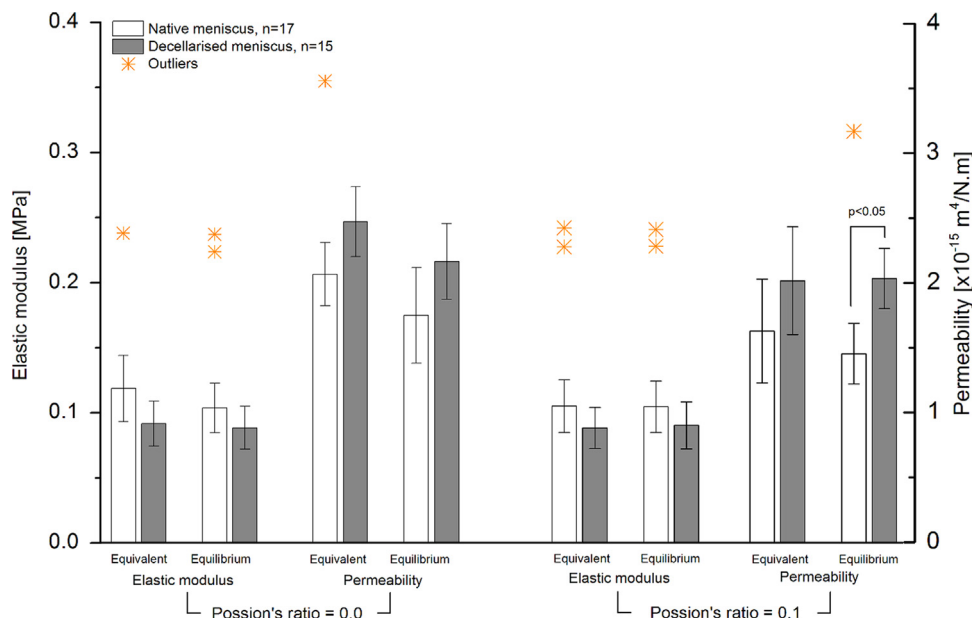|		1.5 mm Specimens ($n=16$)		3.0 mm Specimens ($n=12$)	
		E (MPa)	Permeability $\times 10^{-15}$ m^4/N s	E (MPa)	Permeability $\times 10^{-15}$ m^4/N s
Native	Equivalent	0.24 ± 0.04	3.74 ± 0.97	0.26 ± 0.07	4.74 ± 1.69
	Equilibrium	0.19 ± 0.05	2.06 ± 0.49	0.29 ± 0.08	3.73 ± 1.01
Decellularised	Equivalent	0.18 ± 0.02	4.74 ± 0.61	0.25 ± 0.06	4.14 ± 1.34
	Equilibrium	0.13 ± 0.02	2.73 ± 0.52	0.29 ± 0.06	4.04 ± 1.38

Fig. 6. Unconfined compression biomechanical properties for native and decellularised porcine menisci (mean $\pm$ 95% CI), for 3.0 mm thickness meniscal pins and 0.01 MPa stress.

The tensile study showed that the tensile biomechanical properties of native porcine meniscus are cross-sectional area and position dependent (Fig. 3). This dependence can be explained by the nature of the collagen fibre arrangement in the structure of the meniscus, with different regions having different arrangements with varied fibre densities and orientations (Fithian et al., 1990; Mcdermott et al., 2008; Fox et al., 2012). Similar dependence relationships of the meniscal tensile biomechanical properties on the cross-sectional area, specimen location and direction have been reported in the literature (Proctor et al., 1989; Fithian et al., 1990; Lechner et al., 2000; Leroux and Setton, 2002; Mcdermott et al., 2008). The $1.5 \times 1.5 \times 10$ [mm] specimens had the highest initial elastic modulus. This might have been due the high pre-stress associated with this small cross-sectional area due to the preload.

The decellularised medial porcine meniscal tensile properties were compared to the corresponding native meniscal properties (Fig. 4), using the 3×3 [mm] cross-sectional area to describe the overall structure of the tissue. The decellularisation process appeared to decrease the initial elastic modulus (ANOVA, $p < 0.05$) compared to that of native porcine meniscus. However, further microscopic and histology studies are required to investigate this effect. The reported average range for the human meniscal circumferential tensile elastic modulus and ultimate tensile strength ranges between 50 and 198 [MPa] (Tissakht and Ahmed, 1995; Lechner et al., 2000; Leroux and Setton, 2002) and between 8 and 19 [MPa] (Bullough et al., 1970; Fithian et al., 1990; Tissakht and Ahmed, 1995), respectively, depending on the specimens location, region, and dimensions. The corresponding average values for decellularised medial porcine meniscus from the current study were 133 MPa and 35 MPa, respectively.

The experimental indentation and unconfined compression creep studies were carried out to determine the compressive biomechanical properties of native and decellularised menisci. For the native porcine meniscus, the reported average compressive elastic modulus and permeability were 0.27 ± 0.04 MPa and $1.74 \times 10^{-15} \pm 0.19 \times 10^{-15}$ m^4/N s (from confined compression test, 1.10 mm thickness specimens) (Joshi et al., 1995) and 0.13 ± 0.03 MPa and $6.32 \times 10^{-15} \pm 4.21 \times 10^{-15}$ m^4/N s (from indentation creep test, whole specimens) (Sweigart et al., 2004), respectively, whereas the results presented here were 0.29 ± 0.08 MPa and $3.73 \times 10^{-15} \pm 1.01 \times 10^{-15}$ m^4/N s (indentation, 3 mm specimens). These differences between the results presented here and the reported results for native porcine meniscus are most likely due to differences in test type, test conditions, solution techniques, specimen size, direction and location (Joshi et al., 1995; Sweigart et al., 2004).

The reported compressive elastic modulus and permeability for human meniscus ranged between 0.09 and 0.23 [MPa] and from 1.32×10^{-15} to 2.74×10^{-15} m^4/N s, respectively, depending on test type and conditions (Joshi et al., 1995; Sweigart et al., 2004). The reported wide range of biomechanical properties for human tissue can attributed to the dependence of the biomechanical properties on the age of the donor, test conditions, and specimen specifications. The predicted compressive elastic modulus and permeability for decellularised meniscus reported here of between 0.09 and 0.29 [MPa] and between 2.47×10^{-15} and 4.74×10^{-15} m^4/N s, respectively, were within the corresponding reported range for human meniscus.

This is the first study to investigate the effects of a decellularisation process on both the tensile and compressive biomechanical properties of the porcine medial meniscus. The results suggested that the decellularisation process had some degree of effect on the biomechanical tensile and compressive properties of the porcine medial meniscus. The basic study by Stapleton et al. indicated similar results (Stapleton et al., 2008), which reported insignificant $\sim 10\%$ increase in the decellularised meniscus tensile elastic modulus, ultimate tensile strength, transition stress and 33% increase in transition strain (ANOVA, $p > 0.05$, $n = 7$), compared to native

meniscus. In addition, in their indentation study, the native and decellularised menisci showed similar deformation under 0.14 MPa stress (ANOVA, $p > 0.05$, $n = 6$), and $\sim 6\%$ increase in the decellularised meniscus deformation under 0.28 MPa, compared to native meniscus (ANOVA, $p > 0.05$, $n = 3$). However, the tensile study was performed at 10 times higher strain rate than the current study, and computational simulation was not adopted to predict the compressive biomechanical properties of the tissue (Stapleton et al., 2008).

The current study showed that decellularised porcine medial meniscus maintained the tensile biomechanical properties of the native meniscus, but had a lower initial elastic modulus. The decellularised porcine medial meniscus generally showed lower compressive elastic modulus and higher compressive permeability compared to that of native meniscus. These changes in the biomechanical properties were most likely due the reduction in glycosaminoglycan (GAG) content during decellularisation. The previously reported histological, immunohistochemical, and biochemical analyses showed that the decellularised tissue retained the major structural proteins, however, there was approximately 60% loss of GAG content. This GAG loss was location dependent and varied from zero to 100% GAG loss, with the central area maintained its GAG content (Stapleton et al., 2008). The GAG content is known to be directly related to the compressive biomechanical properties of the tissue. As the wide 8 mm diameter meniscal pins were cut from the central portion of the tissue, the compressive test specimens represent the average of the GAG content and the average of the changes in GAG content. However, the effect of different positions in the meniscus on GAG content and changes in GAG content will be studied further in the future. The predicted changes in the compressive biomechanical properties were not significant in the majority of the comparisons. In addition, the predicted tensile and compressive biomechanical properties for the decellularised porcine medial meniscus were within the reported range for the human meniscus (Bullough et al., 1970; Fithian et al., 1990; Joshi et al., 1995; Tissakht and Ahmed, 1995; Sweigart et al., 2004).

The limitations associated with the linear biphasic theory and constant permeability assumptions are well recognised. In addition, Poisson's ratio was assumed in the unconfined compression study (either zero or 0.1). It was however difficult to measure the deformation in the lateral direction in order to calculate Poisson's ratio. Moreover, the tensile and compressive biomechanical properties of human meniscus were taken from the literature, rather than testing the human meniscus under the same test conditions. These limitations did not affect the main objective of the current study (to investigate the effects of decellularisation on the biomechanical properties of the porcine medial meniscus). Future work will consider testing of the human meniscus under the same test conditions as well as extending the tests to consider confined compression and tensile suture retention tests.

5. Conclusion

The current study documented the differences in the biomechanical properties between native and decellularised medial porcine menisci. A decellularised scaffold derived from the porcine medial meniscus maintained the tensile biomechanical properties of the native meniscus, but had a lower initial elastic modulus. The decellularised porcine medial meniscus generally showed lower elastic modulus and higher permeability under compression, compared to that of native meniscus. These changes in the biomechanical properties of porcine medial meniscus were attributed to the reduction of GAG content during decellularisation. The predicted biomechanical properties of decellularised medial porcine meniscus were however within the reported range for the human meniscus. The decellularised

porcine meniscus therefore has potential as a partial meniscus replacement device.

Conflict of interest statement

J. Fisher is a consultant to DePuy Synthes UK, and share holder of Tissue Regenix plc.

E. Ingham is a consultant to and share holder of Tissue Regenix plc.

Acknowledgments

References

Aagaard, H., Verdonk, R., 1999. Function of the normal meniscus and consequences of meniscal resection. Scand J. Med. Sci. Sports 9, 134–140.

Abd Latif, M.J., JIN, Z., Wilcox, R.K., 2012. Biomechanical characterisation of ovine spinal facet joint cartilage. J. Biomech. 45, 1346–1352.

Ahmed, A.M., Burke, D.L., 1983. In-vitro of measurement of static pressure distribution in synovial joints—Part I: Tibial surface of the knee. J. Biomech. Eng. 105, 216–225.

Ahmed, A.M., Burke, D.L., Yu, A., 1983. In-vitro measurement of static pressure distribution in synovial joints—Part II: Retropatellar surface. J. Biomech. Eng. 105, 226–236.

Allen, A.A., Caldwell, JR, G. L., Fu, F.H., 1995. Anatomy and biomechanics of the meniscus. Oper. Tech. Orthop. 5, 2–9.

Allen, C.R., Wong, E.K., Livesay, G.A., Sakane, M., fu, F.H., Woo, S.L.Y., 2000. Importance of the medial meniscus in the anterior cruciate ligament-deficient knee. J. Orthop. Res. 18, 109–115.

Andrews, S., Shrive, N., Ronsky, J., 2011. The shocking truth about meniscus. J. Biomech. 44, 2737–2740.

Armstrong, C., Lai, W., Mow, V., 1984. An analysis of the unconfined compression of articular cartilage. J. Biomech. Eng. (106), 165–173.

Athanasiou, K.A., Rosenwasser, M.P., Buckwalter, J.A., Malinin, T.I., Mow, V.C., 1991. Interspecies comparisons of in situ intrinsic mechanical properties of distal femoral cartilage. J. Orthop. Res. 9, 330–340.

Baratz, M.E., Fu, F.H., Mengato, R., 1986. Meniscal tears: the effect of meniscectomy and of repair on intraarticular contact areas and stress in the human knee: a preliminary report. Am. J. Sports Med. 14, 270–275.

Bullough, P.G., Munuera, L., Murphy, J., Weinstein, A.M., 1970. The strength of the menisci of the knee as it relates to their fine structure. J. Bone Joint Surg. Br. 52, 564–570.

Chia, H.N., Hull, M., 2008. Compressive moduli of the human medial meniscus in the axial and radial directions at equilibrium and at a physiological strain rate. J. Orthop. Res. 26, 951–956.

Englund, M., Roos, E.M., Lohmander, L.S., 2003. Impact of type of meniscal tear on radiographic and symptomatic knee osteoarthritis: a sixteen-year followup of meniscectomy with matched controls. Arthritis Rheum. 48, 2178–2187.

Faivre, B., Boisrenoult, P., Lonjon, G., Pujol, N., Beaufils, P., 2014. Lateral meniscus allograft transplantation: clinical and anatomic outcomes after arthroscopic implantation with tibial tunnels versus open implantation without tunnels. Orthop. Traumatol.: Surg. Res. 100, 297–302.

Fithian, D.C., Kelly, M.A., Mow, V.C., 1990. Material properties and structure–function relationships in the menisci. Clin. Orthop. Relat. Res. 252, 19–31.

Fox, A.J., Bedi, A., Rodeo, S.A, 2012. The basic science of human knee menisci structure, composition, and function. Sports Health: A Multi. Approach 4, 340–351.

Fukubayashi, T., Kurosawa, H., 1980. The contact area and pressure distribution pattern of the knee: a study of normal and osteoarthrotic knee joints. Acta Orthop. 51, 871–879.

Goertzen, D., Budney, D., Cinats, J., 1997. Methodology and apparatus to determine material properties of the knee joint meniscus. Med. Eng. Phys. 19, 412–419.

Hayes, W., Keer, L., Herrmann, G., Mockros, L., 1972. A mathematical analysis for indentation tests of articular cartilage. J. Biomech. 5, 541–551.

Hori, R.Y., Mockros, L., 1976. Indentation tests of human articular cartilage. J. Biomech. 9, 259–268.

Huang, H., Zhang, J., Sun, K., Zhang, X., Tian, S., 2011. Effects of repetitive multiple freeze–thaw cycles on the biomechanical properties of human flexor digitorum superficialis and flexor pollicis longus tendons. Clin. Biomech. 26, 419–423.

James, E., Laprade, C., Feagin, J., Laprade, R., 2014. Repair of a complete radial tear in the midbody of the medial meniscus using a novel crisscross suture transtibial tunnel surgical technique: a case report. Knee Surg., Sports Traumatol., Arthroscopy, 1–6.

Jin, Z.M., Pickard, J.E., Forster, H., Ingham, E., Fisher, J., 2000. Frictional behaviour of bovine articular cartilage. Biorheology 37, 57–63.

Joshi, M.D., Suh, J.K., Marui, T., Woo, S.L.Y., 1995. Interspecies variation of compressive biomechanical properties of the meniscus. J. Biomed. Mater. Res. 29, 823–828.

Kainer, M.A., Linden, J.V., Whaley, D.N., Holmes, H.T., Jarvis, W.R., Jernigan, D.B., Archibald, L.K., 2004. Clostridium infections associated with musculoskeletal-tissue allografts. N. Engl. J. Med. 350, 2564–2571.

Kon, E., Chiari, C., Marcacci, M., Delcogliano, M., Salter, D.M., Martin, I., Ambrosio, L., Fini, M., Tschon, M., Tognana, E., 2008. Tissue engineering for total meniscal substitution: animal study in sheep model. Tissue Eng. Part A 14, 1067–1080.

Kon, E., Filardo, G., Tschon, M., Fini, M., Giavaresi, G., Reggiani, L.M., Chiari, C., Nehrer, S., Martin, I., Salter, D.M., 2012. Tissue engineering for total meniscal substitution: animal study in sheep model—results at 12 months. Tissue Eng. Part A 18, 1573–1582.

Kurosawa, H., Fukubayashi, T., Nakajima, H., 1980. Load-bearing mode of the knee joint: physical behavior of the knee joint with or without menisci. Clin. Orthop. Relat. Res. 149, 283–290.

Laible, C., Stein, D.A., Kiridly, D.N., 2013. Meniscal repair. J. Am. Acad. Orthop. Surg. 21, 204–213.

Lechner, K., Hull, M., Howell, S., 2000. Is the circumferential tensile modulus within a human medial meniscus affected by the test sample location and cross sectional area? J. Orthop. Res. 18, 945–951.

Leroux, M.A., Setton, L.A., 2002. Experimental and biphasic FEM determinations of the material properties and hydraulic permeability of the meniscus in tension. J. Biomech. Eng. 124, 315–321.

Lynch, H.A., Johannessen, W., Wu, J.P., Jawa, A., Elliott, D.M., 2003. Effect of fiber orientation and strain rate on the nonlinear uniaxial tensile material properties of tendon. J. Biomech. Eng. 125, 726–731.

Maroudas, A., Bullough, P., Swanson, S., Freeman, M., 1968. The permeability of articular cartilage. J. Bone Joint Surg. Br. 50, 166–177.

Marsano, A., Vunjak-Novakovic, G., Martin, i. Towards tissue engineering of meniscus substitutes: selection of cell source and culture environment. In: 28th Annual International Conference of the IEEE Engineering in Medicine and Biology Society, 2006, EMBS '06., Aug. 30–Sept. 3 2006, pp. 3656–3658.

Mcdermott, I.D., Amis, A.A., 2006. The consequences of meniscectomy. J. Bone Joint Surg. Br. 88-B, 1549–1556.

Mcdermott, I.D., Masouros, S.D., Amis, A.A., 2008. Biomechanics of the menisci of the knee. Curr. Orthop. 22, 193–201.

Milachowski, K., Weismeier, K., Wirth, C., 1989. Homologous meniscus transplantation. Int. Orthop. 13, 1–11.

Moriguchi, Y., Tateishi, K., Ando, W., Shimomura, K., Yonetani, Y., Tanaka, Y., Kita, K., Hart, D.A., Gobbi, A., Shino, K., Yoshikawa, H., Nakamura, N., 2013. Repair of meniscal lesions using a scaffold-free tissue-engineered construct derived from allogenic synovial MSCs in a miniature swine model. Biomaterials 34, 2185–2193.

Muscolo, D.L., Costa-Paz, M., Ayerza, M., Makino, A., 2006. Medial meniscal tears and spontaneous osteonecrosis of the knee. Arthroscopy: J. Arthroscopic Relat. Surg. 22, 457–460.

Papalia, R., Franceschi, F., Diaz Balzani, L., d'Adamio, S., Maffulli, N., Denaro, V., 2013. Scaffolds for partial meniscal replacement: an updated systematic review. Br. Med. Bull.

Pawaskar, S.S., Fisher, J., Jin, Z., 2010. Robust and general method for determining surface fluid flow boundary conditions in articular cartilage contact mechanics modeling. J. Biomech. Eng. 132, 031001.

Proctor, C., Schmidt, M., Whipple, R., Kelly, M., Mow, V., 1989. Material properties of the normal medial bovine meniscus. J. Orthop. Res. (7), 771–782.

Rizzi, R., Bearzi, C., Mauretti, A., Bernardini, S., Cannata, S., Gargioli, C., 2012. Tissue engineering for skeletal muscle regeneration. Muscles, Ligaments Tendons J. 2, 230.

Rongen, J.J., van Tienen, T.G., van Bochove, B., Grijpma, D.W., Buma, P., 2014. Biomaterials in search of a meniscus substitute. Biomaterials 35, 3527–3540.

Stapleton, T.W., Ingram, J., Katta, J., Knight, R., Korossis, S., Fisher, J., Ingham, E., 2008. Development and characterization of an acellular porcine medial meniscus for use in tissue engineering. Tissue Eng. Part A 14, 505–518.

Stensrud, S., Risberg, M.A., Roos, E.M., 2014. Knee function and knee muscle strength in middle-aged patients with degenerative meniscal tears eligible for arthroscopic partial meniscectomy. Br. J. Sports Med. 48, 784–788.

Stollsteimer, G.T., Shelton, W.R., Dukes, A., Bomboy, A.L., 2000. Meniscal allograft transplantation: A 1- to 5-year follow-up of 22 patients. Arthroscopy: J. Arthroscopic Relat. Surg. 16, 343–347.

Sweigart, M., zhu, c., burt, d., agrawal, c., clanton, t., athanasiou, k., 2004. Intraspecies and interspecies comparison of the compressive properties of the medial meniscus. Ann. Biomed. Eng. 32, 1569–1579.

Tissakht, m., ahmed, a., 1995. Tensile stress–strain characteristics of the human meniscal material. J. Biomech. 28, 411–422.

Tugwell, B.D., Patel, P.R., Williams, I.T., Hedberg, K., Chai, F., Nainan, O.V., Thomas, A.R., Woll, J.E., Bell, B.P., Cieslak, P.R., 2005. Transmission of hepatitis C virus to several

organ and tissue recipients from an antibody-negative donor. Ann. Intern. Med. 143, 648–654.

Voloshin, A.S., Wosk, J., 1983. Shock absorption of meniscectomized and painful knees: a comparative in vivo study. J. Biomed. Eng. 5, 157–161.

Vundelinckx, B., Vanlauwe, J., Bellemans, J., 2014. Long-term subjective, clinical, and radiographic outcome evaluation of meniscal allograft transplantation in the knee. Am. J. Sports Med. 0363546514530092.

Wirth, C.J., Peters, G., Milachowski, K.A., Weismeier, K.G., Kohn, D., 2002. Long-term results of meniscal allograft transplantation. Am. J. Sports Med. 30, 174–181.

Yahia, L., Zukor, D., 1994. Irradiated meniscal allotransplants of rabbits: study of the mechanical properties at six months postoperation. Acta Orthop. Belg. 60, 210–215.

Yoon, K.H., Lee, S.H., Park, S.Y., Kim, H.J., Chung, K.Y., 2014. Meniscus allograft transplantation: a Comparison of medial and lateral procedures. Am. J. Sports Med. 42, 200–207.